

## Article

# In Vitro Radioenhancement Using Ultrasound-Stimulated Microbubbles: A Comparison of Suspension and Adherent Cell States

Giulia McCorkell <sup>1</sup>, Masao Nakayama <sup>1,2</sup>, Bryce Feltis <sup>3</sup>, Terrence J. Piva <sup>3,\*</sup> and Moshi Geso <sup>1,\*</sup>

- <sup>1</sup> Discipline of Medical Radiations, School Health and Biomedical Sciences, RMIT University, Bundoora, VIC 3083, Australia; giulia.mccorkell2@rmit.edu.au (G.M.); naka2008@med.kobe-u.ac.jp (M.N.)
- <sup>2</sup> Division of Radiation Oncology, Kobe University Graduate School of Medicine, 7-5-2 Kusunokicho, Kobe 650-0017, Japan
- <sup>3</sup> Discipline of Human Bioscience, School of Health and Biomedical Sciences, RMIT University, Bundoora, VIC 3083, Australia; brycenf@gmail.com
- \* Correspondence: terry.piva@rmit.edu.au (T.J.P.); moshi.geso@rmit.edu.au (M.G.)

**Simple Summary:** This study explores the potential of using ultrasound-stimulated microbubbles (USMB) to enhance the radiation treatment of cancer. We investigated how the condition of the cells being studied (i.e., whether they were adhered or freely floating in suspension) affected the effectiveness of USMB in enhancing radiation therapy. Two types of cancer cells—one primary and one metastatic—were treated with microbubbles and ultrasound followed by different doses of X-ray radiation. The results showed significant differences depending on the cell culture state and cell type. An additive effect was observed for all radiation dose levels in the primary cancer cell line when cells were treated in suspension, whereas this effect was only observed at higher doses in the metastatic cell line. This study provides valuable insights into how cell type and culture conditions can impact the potential benefits of USMB in enhancing radiation treatment for cancer.



**Citation:** McCorkell, G.; Nakayama, M.; Feltis, B.; Piva, T.J.; Geso, M. In Vitro Radioenhancement Using Ultrasound-Stimulated Microbubbles: A Comparison of Suspension and Adherent Cell States. *Radiation* **2023**, *3*, 153–164. <https://doi.org/10.3390/radiation3030013>

Academic Editor: Gabriele Multhoff

Received: 1 June 2023

Revised: 24 July 2023

Accepted: 4 August 2023

Published: 10 August 2023



**Copyright:** © 2023 by the authors. Licensee MDPI, Basel, Switzerland. This article is an open access article distributed under the terms and conditions of the Creative Commons Attribution (CC BY) license (<https://creativecommons.org/licenses/by/4.0/>).

**Abstract:** Background: Ultrasound-stimulated microbubbles (USMB) have shown potential for enhancing radiation treatment via cavitation and sonoporation mechanisms. However, in vitro studies have produced inconsistent results, with adherent cells demonstrating no radioenhancement. This study aims to investigate the effect of cell adherence on in vitro radioenhancement using USMB and radiation. Method: Lung metastases of follicular thyroid carcinoma cells (FTC-238) and non-small cell lung carcinoma cells (NCI-H727) were treated, both when adhered and in suspension, using 1.6% (*v/v*) Definity™ microbubbles, ~90 s of 2 MHz ultrasound with mechanical index 0.9, and either 3 Gy or 6 Gy of megavoltage (MV) X-rays. The cell viability was measured using an MTS assay 72 h post-treatment, and statistical analysis was conducted using a three-way analysis of variance. Results: Statistically significant differences were observed for cells treated when adherent compared to suspended. An additive effect was detected in NCI-H727 cells treated in suspension, but not while adherent, while no enhancement was observed for FTC-238 cells in either culture state. Conclusions: To the best of our knowledge, this is the first study to directly compare the effect of cell adherence on the radioenhancement potential of USMB in vitro, and the first to do so using a metastatic cell line.

**Keywords:** ultrasound; microbubbles; radiation; culture state

## 1. Introduction

Ultrasound-stimulated microbubbles (USMB) have recently been shown to enhance the effects of radiation treatments (RT). Czarnota et al. [1] first reported significant increases in mean animal survival from 19 to 28 days in PC3 human prostate cancer xenografted mice exposed to 24 Gy in 12 fractions of RT in combination with USMB (USMB+RT) compared to those exposed to RT alone. Daecher et al. [2] also reported an increase

in mean animal survival from 11 days using RT alone, to 35 days for USMB+RT, for human hepatocellular carcinoma xenografts in nude rats treated with a single dose of 5 Gy radiation. These enhancements are thought to be produced as a result of cavitation effects on the tumour cells, triggering the upregulation of acid sphingomyelinase (ASMase) to hydrolyse sphingomyelin into ceramide, which is in turn associated with apoptotic cell death [3]. In stable cavitation, acoustic pressures from the applied ultrasound (US) field cause microbubbles (MBs) to expand and contract in a symmetrical manner, with their diameters fluctuating in response to rarefactions and compressions of the applied US field. The resulting fluid disturbances in the extracellular space cause sheer stress on the cell, along with direct push/pull effects of MBs on the plasma membrane and penetration of the lipid bilayer [4]. Higher US pressures can lead to inertial cavitation, where MBs rupture, triggering shock waves and microjets from their asymmetrical collapse, resulting in the puncturing of cell membranes in a process termed sonoporation. The potential to harness both these cavitation and sonoporation effects for therapeutic applications has been the subject of much research [5–11].

One of the main challenges with the study of these effects is the myriad of parameters used by researchers across the large number of variables involved, such as differences in US settings; MB types and concentrations; cell lines or tumour types; and extracellular environments [12]. For *in vitro* studies specifically, adherent or suspension cell culture states have also been found to influence results. Kinoshita and Hynynen [13] observed decreased viability of suspended RatC166 cells exposed to USMB compared to those that were adherent, despite observing similar levels of sonoporation efficacy in both states. However, two further studies by Zhang et al. [14] and Zhou et al. [15] using mouse embryonic fibroblasts and 293T cells, respectively, reported greater increases in both cell viability and sonoporation efficiency for suspended cells compared to adherent cells.

In the context of radioenhancement using USMB, biophysical cavitation effects have been leveraged alongside sonoporation effects to facilitate the role of MBs as treatment vectors in increasing the cellular uptake of drugs or genes *in vivo*. Ultrasound-stimulated oxygen microbubbles (USMBO) and RT were used to treat MDA-MB-231 human adenocarcinoma breast cells in mice [16]. A significant growth delay was seen using USMBO+RT when compared to that seen when these cells were treated with either USMBO or US+RT. The sonoporation effects increased intratumoural oxygenation levels prior to RT, thereby overcoming one of the main limitations of RT in tumour hypoxia. Nande et al. [17] treated DU-145 prostate cancer xenografts in mice with 16 Gy in two fractions of radiation, with and without USMBs, loaded with p53 genes (USMBp53). A significant increase in growth inhibition at 19 weeks post-treatment was observed for cells treated with USMBp53+RT (~94%) compared to that with RT alone (~22%).

However, *in vitro* studies using USMB+RT have shown some inconsistent results. Several studies involving exploring USMB radiosensitisation of human umbilical vein Endothelial Cells (HUVEC), Acute Myeloid Leukaemia Cells (AML-5), Human prostate cancer cells (PC3) and murine fibrosarcoma cells (KHT-C) all demonstrated increases in *in vitro* cell death for cells treated with USMB+RT compared to RT-alone [18–22]. However, Lammertink et al. [23] observed no discernible difference in the cell survival curves between RT alone and USMB+RT for human pharyngeal squamous cells (FaDu), suggesting that the cavitation effects of USMB on their own do not elicit any radioenhancement—a finding that stands in stark contrast to all other results reported to date [24,25]. This was also the only *in vitro* study to expose adherent cells to USMB+RT, which raises the question of whether *in vitro* radiosensitisation using USMB is influenced by cell state.

To investigate this further, we extended our previous *in vitro* research to two new cell lines that had not been explored before were treated in a suspended state using USMB+RT, and we observed a dose enhancement compared to those cells only treated with RT [26]. In this present study, we treated the same lung metastasis of follicular thyroid carcinoma cells (FTC-238) and non-small cell lung carcinoma cells (NCI-H727) in an adherent state, and

compared the results with our previous findings to investigate the influence of cell culture state on in vitro radioenhancement using ultrasound-stimulated microbubbles.

## 2. Materials and Methods

### 2.1. Cell Lines and Culture Conditions

As described previously, all of the experiments were performed using FTC-238 and NCI-H727 cells [26]. These cells were supplied by the European Collection of Cell Cultures (ECACC; Salisbury, UK) as catalogue numbers 94,060,902 and 94,060,303, respectively, and were purchased from CellBank Australia (Westmead, NSW, Australia). Both cell lines have previously been described [27–29], and were maintained according to manufacturer's instructions and grown under aseptic conditions at 37 °C, 5% CO<sub>2</sub> and 95% humidity. The FTC-238 cells were cultured using DMEM:F12 (Sigma-Aldrich, catalogue number D8437), supplemented with 5% foetal bovine serum (FBS) (Corning, catalogue, 35-076-CV supplied by Fisher Biotec, Victoria, Australia) and 1% penicillin–streptomycin (Sigma-Aldrich, catalogue number 15070063). The NCI-H727 cells were cultured in RPMI 1640 (Thermo Fisher, catalogue number 11875093), supplemented with 10% FBS and 1% penicillin–streptomycin.

### 2.2. Plating and MTS Assay Optimisation

To each T12.5 cm<sup>2</sup> tissue culture flask (Bio-Strategy, catalogue BDAA353107), 7500 FTC-238 and 60,000 NCI-H727 cells were plated. The cell seeding densities were optimised prior to achieve 80% confluence at 72 h post-treatment, as measured by the CellTiter 96<sup>®</sup> Aqueous One Solution cell proliferation assay (Promega, catalogue number G3582). The MTS tetrazolium compound (3-(4,5-dimethylthiazol-2-yl)-5-(3-carboxymethoxyphenyl)-2-(4-sulfophenyl)-2H-tetrazolium) was bio-reduced by viable cells into a coloured formazan product that could be analysed via colorimetry [30]. Eight flasks for each cell line were allowed to adhere overnight for ~14–16 h prior to treatment. Each experiment was performed in triplicate, with separate experiments run for each cell line, resulting in 6 experiments in total.

### 2.3. Treatments

Two hours prior to treatment, the flasks were filled to a total volume of 30 mL using cell-line specific media. Definity<sup>®</sup> perflutren lipid microspheres (mean diameter 1.3–3.3 µm) (Lantheus Medical Imaging, Inc., supplied by Global Medical Solutions, Melbourne, VIC, Australia) were activated using the Vialmix<sup>®</sup> activation device (Lantheus Medical Imaging, Inc.) following the manufacturer's instructions [31], and 480 µL was added to the relevant treatment flasks to give a final microbubble concentration of 1.6% (*v/v*) [26]. The flasks were then transported offsite to the treatment facility at the Genesis Care Epping Radiation Oncology Centre (EPROC) (Epping, VIC, Australia). The travel time to and from the treatment facilities was around 20 min each way, with the cells out of the incubator for ~90 min overall.

Once onsite, ultrasound sonication was applied using the LOGIQ i portable ultrasound with the 4C-RS transducer (GE Healthcare, Chicago, IL, USA). Ultrasound (2 MHz frequency) was applied directly to the flask using a coupling gel, with a focal point of 3.25 cm focal point and a depth of 4 cm used to achieve a mechanical index of 0.9, as per our previous study [26]. The transducer was moved across the flask for approximately 90 s until the opaque, milky-white microbubbles had burst, and the media had returned to its normal transparency (Figure 1). Three control flasks were left untreated, whilst the USMB-alone-treated flask received ultrasound sonication in the absence of radiation.

X-rays at 6 MV were delivered using a Varian iX linear accelerator. The flasks were laid flat on the treatment couch on top of 10 cm of solid water, with a source-to-surface distance (SSD) of 100 cm set to the top of the solid water from a gantry angle of 0°. For the cells in suspension, an additional 2 cm of solid water was placed on top of the flasks to act as a radiation dose build-up region. For the adherent cells, the cell media in the flasks formed the build-up region given the cells were attached as a monolayer along the bottom

plane of the flask. Both the RT-alone and USMB+RT flasks were irradiated simultaneously using a  $20 \times 20$  cm field size to cover both flasks. A schematic diagram of these setups is shown in Figure 2.

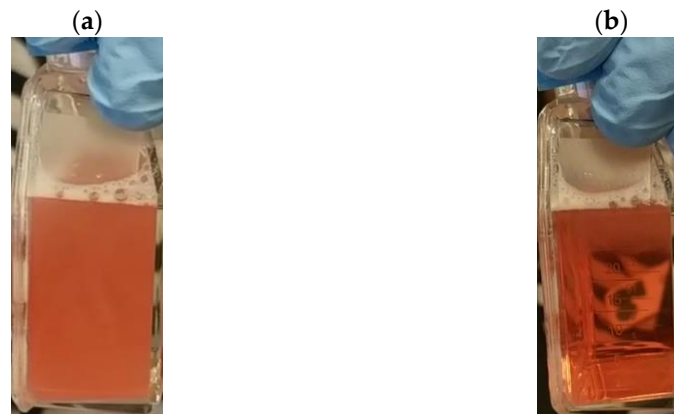


**Figure 1.** Differences in media transparency (a) before and (b) after microbubble stimulation by ultrasound. Flask (a) shows the milky-white translucent appearance of the microbubbles when added to cell culture media at a concentration of 1.6% (*v/v*). Flask (b) shows the cell culture media returned to its normal transparency after a 2 MHz frequency, mechanical index 0.9 ultrasound exposure was applied directly to the flask for ~90 s.

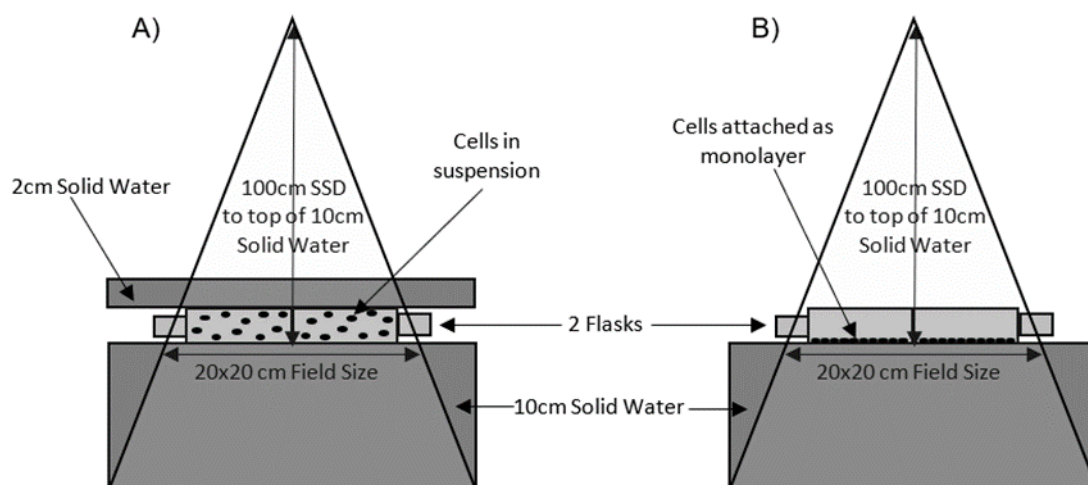


**Figure 2.** Schematic diagram demonstrating experimental setup for MV x-ray exposures of cells in (A) suspension and (B) adherent states. RT-alone and USMB+RT flasks were placed on top of 10 cm solid water, with 100 cm SSD set to top of solid water. For cells treated in suspension, an additional 2 cm of solid water was placed on top of flasks to act as a build-up region. For cells attached as a single monolayer along the flask wall abutting the 10 cm solid water adherent cells, media in the full flasks formed the build-up region. A 6 MV beam was used, with a gantry angle of  $0^\circ$  and a field size of  $20 \times 20$  cm.

Following the treatments, the flasks were transported back to the laboratory. The suspended cells were centrifuged at  $200 \times g$  for 5 min, and resuspended in 10 mL of tissue culture media. For the adherent cells, the treatment compounds and media were discarded and replaced with 10 mL of fresh tissue culture media. All of the cells were then placed in a 5%  $\text{CO}_2$  incubator at  $37^\circ\text{C}$  for 24 h before the tissue culture media was replaced with fresh media and the flasks returned to the incubator.

#### 2.4. MTS Readings

At 72 h post-treatment, the tissue culture media was removed from each flask and replaced with 1 mL of FBS-free tissue culture media and 200  $\mu$ L of MTS at a ratio of 5:1, as per the manufacturer's instructions [30]. Four replicates of 100  $\mu$ L of media and 20  $\mu$ L of MTS were plated in a 96-well plate to serve as media controls. The flasks and plates were then returned to the incubator for 25 min (FTC-238 cells) or 15 min (NCI-H727 cells). Four replicates of 120  $\mu$ L from each flask were then transferred to the 96-well plate, and the absorbance was read at 490 nm on a CLARIOstar Plus Plate reader (BMG Labtech, Mornington, VIC, Australia). The average of these four replicates was calculated for each condition, and an average of the four blank wells subtracted to give the final raw absorbance reading for each condition (flask). Normalised survival was then calculated by dividing these blank-corrected raw absorbance values by the blank-corrected average of the three control (untreated) flasks for each experiment. The results were then averaged across the three experiments, and standard deviations (SD) were calculated.

#### 2.5. Statistical Analysis

Microsoft Excel was used to compile the results and calculate the normalised survival values, as outlined above. The data were then imported into SPSS V26 (International Business Machines Corporation (IBM), Armonk, NY, USA) for the remaining analyses. Statistical significance between treatment groups was tested using a three-way ANOVA  $2 \times 3 \times 2$  design to report on the two levels of USMB (i.e., presence or absence), three radiation dose levels (0, 3 and 6 Gy) and two cell states (adherent and suspension). The key assumptions of the ANOVA test were initially validated using the Shapiro–Wilk (SW) test to confirm the normality of the distributions; and Levine's test was used to confirm homogeneity of error variance and outliers identified visually on the box-and-whisker plot as flagged by SPSS [32,33]. The post hoc analysis included pair-wise *t*-tests, with *p*-values less than 0.05 reported as statistically significant (\*); values between 0.001 to 0.01 as statistically very significant, denoted by \*\*; values between 0.0001 and 0.01 as statistically extremely significant \*\*\*, with any extremely significant values < 0.0001 further denoted as \*\*\*\*. The estimates of effect size were also evaluated using partial eta squared ( $\eta_p^2$ ) as reported by SPSS, with values <0.06 reported as small, values between 0.06 and 0.14 as medium, and values >0.14 as large [34].

### 3. Results

The effect of USMB on the viability of cells exposed in either a suspended or adherent cell culture state was examined using two different cell lines to observe if they directly enhanced radiation-induced cell killing in vitro. A primary non-small cell lung carcinoma (NSCLC) cell line was used (NCI-H727), in addition to a metastatic follicular thyroid carcinoma deposit in lung tissue (FTC-238).

#### 3.1. NCI-H727 Cells

All of the groups contained normally distributed data (Figure 3), as confirmed by SW testing, with no outliers present. We observed significant differences between cells treated in suspension compared to those in an adherent state ( $p < 0.0001$ ). A significant difference in cells treated with, compared to without USMB, was also observed ( $p = 0.004$ ). The partial eta squared values for both these variables were large, with the overall effect size of cell culture state more than double the effect size reported due to the presence or absence of USMB ( $\eta_p^2 = 0.519$  and  $0.204$ , respectively). The two-way interaction of both cell state and presence or absence of USMB together was also highly significant ( $p < 0.0001$ ), demonstrating a large effect size of  $\eta_p^2 = 0.438$ . The radiation dose accounted for the greatest overall effect ( $\eta_p^2 = 0.803$ ); however, a difference in the size of the *p*-values between dose levels was noted, despite both being significant (0 Gy and 3 Gy  $p < 0.0001$ , 3 Gy and 6 Gy  $p = 0.027$ ). Further subgroup analyses of individual conditions revealed statistically significant results across all dose levels for groups of cells treated with USMBs in adherent

compared to suspended cell culture states (Figure 3), as well as cells in suspension treated with compared to without USMBs (Figure 4).

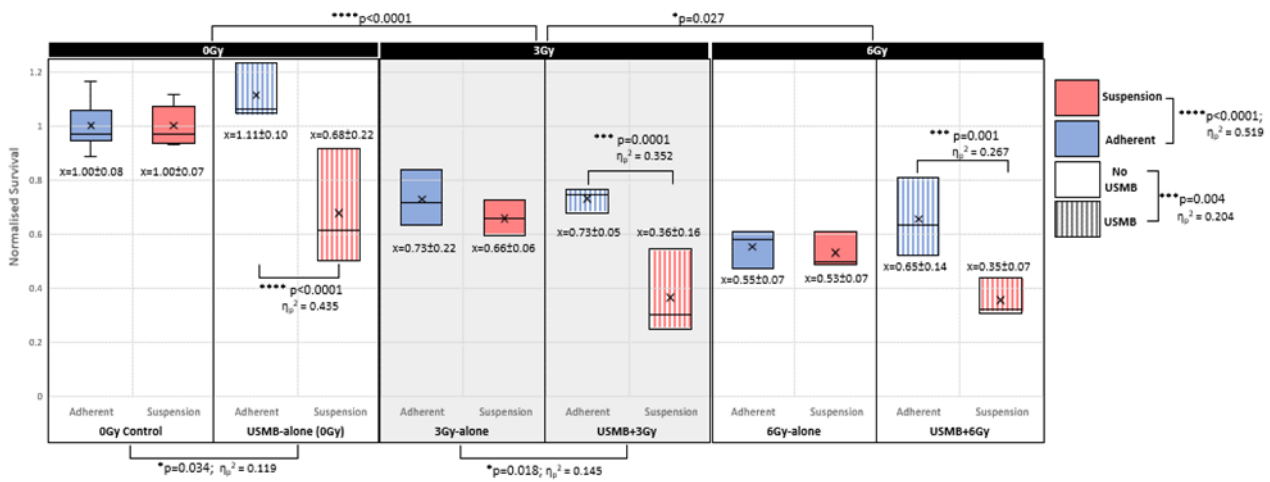


**Figure 3.** Box and whisker plots for NCI-H727 cells, demonstrating the average (cross) and median (middle line) normalised survival, spread of data, and absence of outliers for each treatment condition. Testing via 3-way ANOVA revealed significant differences between all cells treated in suspension compared to adherent cell culture states, as well as all cells treated with compared to without ultrasound-stimulated microbubbles (USMB). Statistically significant overall differences were noted between all cells treated at each of the three radiation dose levels (top of graph). Significant differences were also seen for all cells treated at 0 Gy and 3 Gy with USMB compared to without; however, this was not the case for 6 Gy (bottom of graph). There were also significant differences for cells treated in different cell culture states with USMB at each radiation dose level (patterned red vs. patterned blue shading); however, this was not the case for cells treated with RT alone (plain red vs. plain blue shading). \*  $p < 0.05$ ; \*\*\*  $p < 0.001$ ; \*\*\*\*  $p < 0.0001$ .

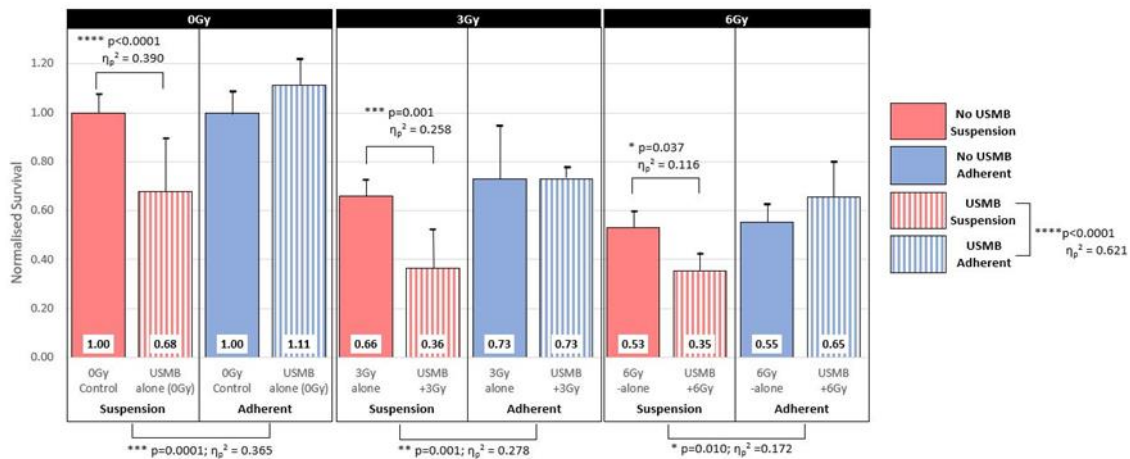


**Figure 4.** Bar chart showing changes to normalised survival of NCI-H727 cells through the addition of USMB (patterned vs. plain shading) for each radiation dose level and different cell state (suspension = red, adherent = blue). Error bars indicate standard deviations for the three biological replicates of each experiment. Significant differences were noted for all cells treated using USMB+RT in suspension. Significant differences were also seen in cells treated in suspension compared to adherent states across all dose levels (bottom of graph). There were also significant differences observed for cells treated in suspension with USMB compared to without, across all dose levels (red plain vs. red patterned shading); however, this was not the case for cells treated in the adherent state (blue plain vs. blue patterned shading). \*  $p < 0.05$ ; \*\*  $p < 0.01$ ; \*\*\*  $p < 0.001$ ; \*\*\*\*  $p < 0.0001$ .

### 3.2. FTC-238 Cells

In the FTC-238 cell datum, SW testing revealed the adherent USMB + 3 Gy subgroup was non-normally distributed ( $p < 0.0001$ ), thereby violating the assumptions required for the 3-way ANOVA test. As this was only the case for one subgroup, and there is literature to support the robustness of the ANOVA to violations of normality, the 3-way ANOVA was still applied with caution in interpreting the results surrounding type I error [35,36].

Significant overall differences between the suspended cells compared to those in an adherent state were observed for this cell type ( $p < 0.014$ ), with a large effect size ( $\eta_p^2 = 0.156$ , Figure 5). The radiation dose accounted for the largest overall effect in the FTC-238 cells, with a value of  $\eta_p^2 = 0.837$ , and the same level of significance was seen across the three dose levels ( $p < 0.0001$  for both 0 Gy and 3 Gy, and as well as 3 Gy and 6 Gy, Figure 5). The combined interaction between radiation dose and cell culture state was significant ( $p = 0.003$ ), and had a larger influence on the results than the cell state alone ( $\eta_p^2 = 0.273$ ). A significant difference and large effect size was observed when the adherent cells were treated with 6 Gy radiation compared to those in a suspended state ( $p = 0.0001$ ,  $\eta_p^2 = 0.341$ ), where no difference or effect was seen at 0 or 3 Gy (Figure 5).

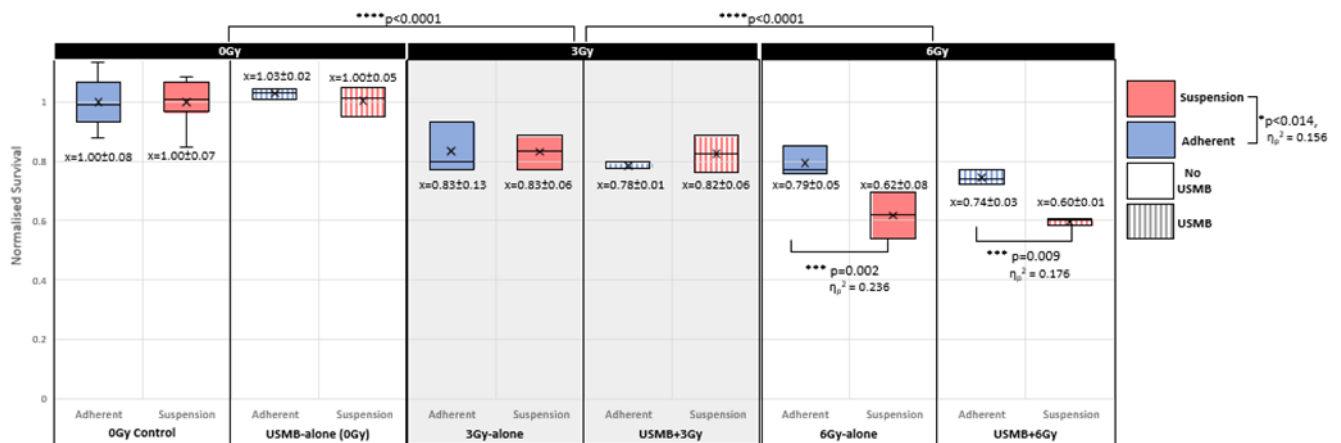


**Figure 5.** Box and whisker plots for FTC-238 cells, demonstrating the average (cross) and median (middle line) normalised survival, spread of data, and absence of outliers for each treatment condition. Testing via 3-way ANOVA revealed statistically significant differences between all cells treated in suspension compared to adherent cell culture states. Significant overall differences were noted between all cells treated at each of the three radiation dose levels (top of graph). Significant differences were also seen for all cells treated in adherent compared to suspension states using 6 Gy-alone (plain red vs. plain blue shading) and USMB + 6 Gy (patterned red vs. patterned blue shading). \*  $p < 0.05$ ; \*\*\*  $p < 0.001$ ; \*\*\*\*  $p < 0.0001$ .

No overall difference was seen between cells treated with compared to without USMB, with only a small effect size of  $\eta_p^2 = 0.015$  observed. Two-way interactions between the radiation dose and the presence or absence of USMB were not significant, despite a small effect size being observed ( $\eta_p^2 = 0.037$ ). There was a significant difference between FTC-238 cells treated with USMB in an adherent state compared to the suspended state ( $p = 0.033$ ), with a medium effect size of  $\eta_p^2 = 0.120$  observed (Figure 6). A small overall effect was seen for the 3-way interaction between radiation dose, cell state and the presence or absence of USMB ( $\eta_p^2 = 0.017$ ); however, this was not significant. Further subgroup analyses revealed two significant results for cells treated in adherent compared to suspension states, using either 6 Gy-alone ( $p = 0.002$ ,  $\eta_p^2 = 0.236$ ) or USMB+6 Gy ( $p = 0.009$ ,  $\eta_p^2 = 0.176$ , Figure 5).

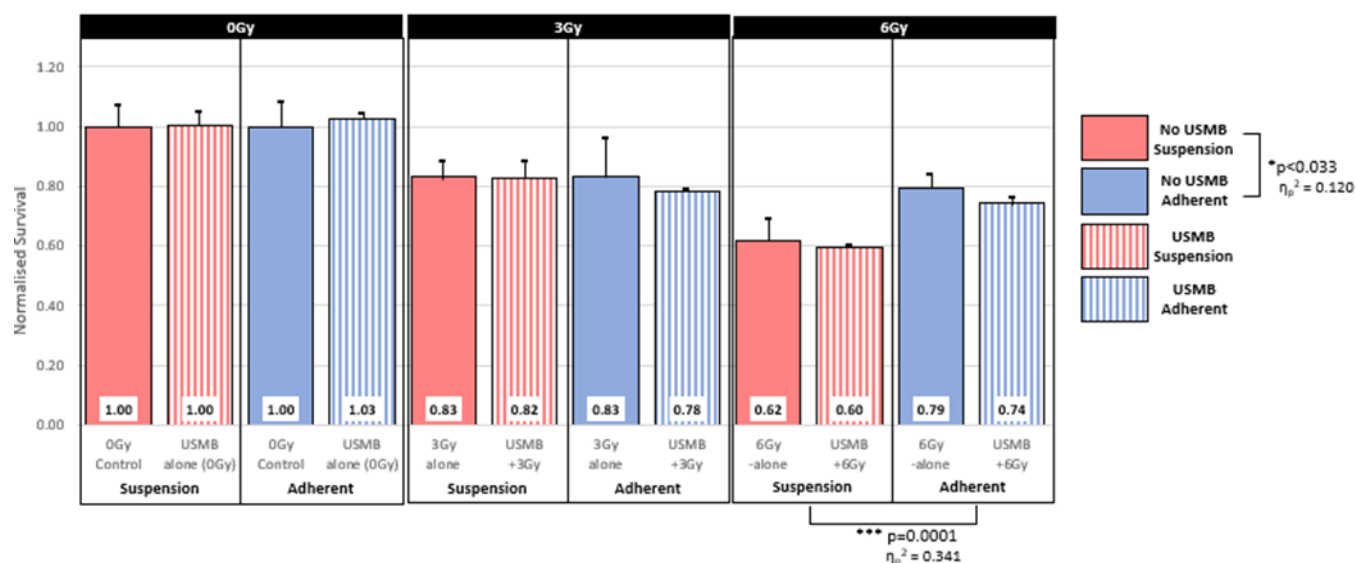


**Figure 6.** Bar chart plot showing any changes to normalised survival of FTC-238 cells through the addition of USMB for each radiation dose level (patterned vs. plain shading) for the different cell states (suspension = red, adherent = blue). Error bars indicate standard deviations for the three biological replicates of each experiment. Significant differences were noted for all cells treated using RT alone in suspension compared to adherent states. A significant difference was also observed between cells treated at 6 Gy in suspension compared to adherent states (bottom of graph, red vs. blue groups). \*  $p < 0.05$ ; \*\*\*  $p < 0.001$ .

#### 4. Discussion

MBs are able to encapsulate various gases, drugs, as well as targeting agents. When used as an ultrasound contrast agent, MBs can act as echo-enhancers and therapeutic agents, and can play an essential role in ultrasound imaging and ultrasound-mediated therapy [37]. USMB therapy is used in treating thrombi, a process called sonothrombolysis [38], nosocomial infections [39], and has been used to transfect cells with DNA [40] as well as trespassing the blood–brain barrier [41]; however, the results of these studies are not conclusive [42]. Most of the research involving USMB has been directed against tumours in vivo to enhance the effects of radiotherapy due to the hypoxic environment found in solid tumours [42].

USMB radioenhancement in vitro is dependent on both cell adherence and cell type. For both cell lines, the overall survival was decreased for suspended cells compared to the adherent cells; however, this was more pronounced for the NCI-H727 cells compared to FTC-238 cells (\*\*\*\*  $p < 0.0001$ ,  $\eta_p^2 = 0.519$  for NCI-H727; \*  $p < 0.014$ ,  $\eta_p^2 = 0.156$  for FTC-238), as seen in Table 1. For the NCI-H727 cells, the magnitude of this effect became less pronounced with increased radiation dose ( $\eta_p^2 = 0.365$ ,  $p = 0.0001$  for 0 Gy;  $\eta_p^2 = 0.278$ ,  $p = 0.001$  for 3 Gy;  $\eta_p^2 = 0.172$ ,  $p = 0.010$  for 6 Gy, Figure 4), whereas for the FTC-238 cells, the effect was greater with increased radiation dose, where a significant difference was seen at 6 Gy ( $\eta_p^2 = 0.0048$ ,  $p = 0.678$  for 0 Gy;  $\eta_p^2 = 0.0055$ ,  $p = 0.659$  for 3 Gy;  $\eta_p^2 = 0.3412$ ,  $p = 0.0001$  for 6 Gy, Figure 5). This suggests that the influence of cell adherence on USMB radiosensitisation in vitro is cell-type dependent. This finding is consistent with data previously described, where varying levels of cell viability and sonoporation efficacy were observed across a range of cell lines exposed to USMB in different cell culture states [13–15].

**Table 1.** Effect of USMB on the viability of irradiated cells treated in both adherent and suspended culture states. The average surviving fraction (normalised to the untreated control for each culture state obtained from the results shown in Figures 3–6) is shown alongside the standard deviation for three biological replicates.

Radiation Dose	Culture State	NCI-H727 Cell Line		FTC-238 Cell Line	
		RT-Alone	USMB + RT	RT-Alone	USMB + RT
0 Gy	Suspended	1.00 ± 0.07	0.68 ± 0.22	1.00 ± 0.07	1.00 ± 0.05
	Adhered	1.00 ± 0.08	1.11 ± 0.10	1.00 ± 0.08	1.03 ± 0.02
3 Gy	Suspended	0.66 ± 0.06	0.36 ± 0.16	0.83 ± 0.06	0.82 ± 0.06
	Adhered	0.73 ± 0.22	0.73 ± 0.05	0.83 ± 0.13	0.78 ± 0.01
6 Gy	Suspended	0.53 ± 0.07	0.35 ± 0.07	0.62 ± 0.08	0.60 ± 0.05
	Adhered	0.55 ± 0.07	0.65 ± 0.14	0.79 ± 0.01	0.74 ± 0.03

#### 4.1. Baseline Sensitivity to USMB In Vitro Is Also Influenced by Cell Adherence

There was a small increase in the proliferation of both cell lines treated with USMB-alone in the adherent state, which was more pronounced for the NCI-H727 cells ( $1.11 \pm 0.05$ ,  $\eta_p^2 = 0.072$ ,  $p = 0.103$ ) than for the FTC-238 cells ( $1.03 \pm 0.02$ ,  $\eta_p^2 = 0.007$ ,  $p = 0.618$ ) compared to the corresponding untreated controls ( $1.00 \pm 0.08$  for both cell lines). A similar increase in survival compared to control was reported for Rat C166 cells treated with USMB in an adherent state compared to untreated controls [13]. A dependence on US parameters and exposure setup, in addition to cell state, was also noted for these cells. The authors did not directly address these results; however, one possible explanation is that low-intensity ultrasound has been associated with tissue regeneration in certain cell types, so it may be possible that under certain US conditions, cell proliferation could be stimulated rather than inhibited [43–45]. Kinoshita et al. also reported decreases in cell viability when cells in vitro were exposed to standing waves, alongside increases in sonoporation efficacy [13]. Given that adherent cells have less capacity to be propagated by ultrasound waves and moved away from the plane of the standing wave than free-floating cells in suspension, they are potentially more susceptible to these effects of the standing wave.

For cells treated with USMB alone in the suspended culture state, there was again no discernible difference in cell survival for the FTC-238 cells compared to untreated controls ( $1.00 \pm 0.05$  compared to  $1.00 \pm 0.07$ ,  $\eta_p^2 < 0.000$ ,  $p = 0.959$ ). However, a significant difference between the NCI-H727 cells in suspension treated with USMB alone compared to untreated control was observed ( $p < 0.0001$ ,  $\eta_p^2 = 0.390$ ), suggesting the interaction between USMB and cells in the different cell culture states may cell-type dependent. This could be related to the fact that in suspension, the entire surface area of the suspended cell is available for USMB–cell interaction, whereas for adherent cells, only some of the cell surface is accessible for USMB interactions due to regions of the membrane being bound to the culture vessel surface. Cells that are more inherently sensitive to the effects of USMB are more likely to be impacted by the increased exposure area than those that are less sensitive, and depending on the degree of sensitivity, these effects may not be seen in the adherent state where the threshold for response may not be exceeded. The concept of cell surface area and MB contact was explored by Zhou et al. [15], who demonstrated it was necessary for effective sonoporation. The results from our study suggest the same may be true for radiosensitisation effects on the cell.

#### 4.2. Baseline Cell Radiosensitivity In Vitro May Also Be Influenced by Cell Adherence

Although not statistically significant, in the absence of USMB, the normalised survival for cells treated with RT alone tended to be lower in the suspended culture state compared to the adherent culture state. For the NCI-H727 cells, this was more pronounced at 3 Gy ( $0.66 \pm 0.06$  SD for cells in treated suspension compared to  $0.73 \pm 0.22$  for adherent cells,  $\eta_p^2 = 0.019$ ,  $p = 0.404$ ) than at 6 Gy ( $0.53 \pm 0.07$  suspension vs.  $0.55 \pm 0.07$  adherent,  $\eta_p^2 = 0.002$ ,  $p = 0.811$ ) (Figure 4). For the FTC-238 cells, the opposite was true, with a significant decrease observed at 6 Gy for suspended cells compared to those that were

adhered ( $0.62 \pm 0.08$  suspension vs.  $0.79 \pm 0.05$  adherent,  $\eta_p^2 = 0.236$ ,  $p = 0.002$ ) (Figure 6). At 3 Gy, there was very little difference in the normalised survival for FTC-238 cells in either culture state ( $0.83 \pm 0.06$  suspension vs.  $0.83 \pm 0.13$  adherent,  $\eta_p^2 < 0.01$ ,  $p = 0.950$ ). This decrease in survival for cells in a suspended compared to an adherent cell culture state may be explained by the phenomenon of anoikis, whereby anchorage-dependent cells undergo apoptosis in response to incorrect cell or extracellular matrix attachment [46]. This effect is highly variable between cell types [46], and metastatic cells have been reported to have increased resistance to anoikis compared to their non-cancerous counterparts [47,48]. This may explain the opposing relationship to radiation dose demonstrated by the different cells, as higher radiation doses of radiation were required to elicit a response in the metastatic cell line.

Taken together, the data presented here are consistent with published research on in vitro sonoporation effects for cells in different cell culture states. This suggests that in vitro radiosensitisation, using USMB is likely influenced by cell adherence, and provides strong evidence to explain the anomalous results reported for FaDu pharyngeal squamous cancer cells [23].

## 5. Conclusions

To the best of our knowledge, this is the first study to directly demonstrate the influence of exposing anchorage-dependent cells to the combination of radiation and USMB in vitro. Anchorage-dependent cells are reported to undergo anoikis induced by the lack of adequate cell or extracellular attachment, with the extent of this determined by cell type. The influence of this was evident in this study, where differences in responses to radiation alone for both cell types treated in suspension were observed. Where NCI-H727 cells in suspension demonstrated differences in cell viability at lower radiation doses compared to those treated in an adherent state, the viability of FTC-238 cells was only impacted at the higher radiation dose. Similar differences were also observed between cells treated using USMB alone compared to untreated controls. FTC-238 cells demonstrated no change in cell viability when treated in an adherent state compared to a suspended state, whereas the viability of NCI-H727 cells significantly decreased when treated in the suspension state compared to the adherent state. Reports that metastatic cells have shown increased resistance to anoikis compared to normal cells offer some explanation for these differences between cell lines, where the FTC-238 metastatic cell line showed no overall dose enhancement using USMB+RT together, compared to NCI-H727 where substantial dose enhancement was observed for cells in suspension, but not in the adherent state. The implications of this study are considerable, given that the bulk of research into the use of USMBs as a radioenhancing agent in vitro primarily exposed cells in suspension.

**Author Contributions:** Conceptualisation, G.M., M.G., B.F. and T.J.P.; data curation, G.M. and M.N.; formal analysis, G.M.; funding acquisition, G.M. and M.G.; investigation, G.M., M.N. and B.F.; methodology, G.M. and B.F.; project administration, G.M. and M.N.; resources, G.M., M.G., B.F. and T.J.P.; supervision, M.G., B.F. and T.J.P.; visualisation, G.M.; writing—original draft, G.M.; writing—review and editing, M.N., M.G., B.F. and T.J.P. All authors have read and agreed to the published version of the manuscript.

**Funding:** This research was funded by the Australian Government's Department of Education and Training under the Joint Research Engagement Engineering Cadetship.

**Institutional Review Board Statement:** Not applicable.

**Informed Consent Statement:** Not applicable.

**Data Availability Statement:** The datasets used and/or analysed during the current study are available from the corresponding author on reasonable request.

**Acknowledgments:** The authors would like to thank the staff at GenesisCare Epping Radiation Oncology Centre for their support and use of their equipment.

**Conflicts of Interest:** The authors declare no conflict of interest.

## References

1. Czarnota, G.J.; Karshafian, R.; Burns, P.N.; Wong, S.; Al Mahrouki, A.; Lee, J.W.; Caissie, A.; Tran, W.; Kim, C.; Furukawa, M.; et al. Tumor radiation response enhancement by acoustical stimulation of the vasculature. *Proc. Natl. Acad. Sci. USA* **2012**, *109*, E2033–E2041. [[CrossRef](#)] [[PubMed](#)]
2. Daecher, A.; Stanczak, M.; Liu, J.-B.; Zhang, J.; Du, S.; Forsberg, F.; Leeper, D.B.; Eisenbrey, J.R. Localized microbubble cavitation-based antivasular therapy for improving HCC treatment response to radiotherapy. *Cancer Lett.* **2017**, *411*, 100–105. [[CrossRef](#)] [[PubMed](#)]
3. El Kaffas, A.; Czarnota, G.J. Biomechanical effects of microbubbles: From radiosensitization to cell death. *Future Oncol.* **2015**, *11*, 1093–1108. [[CrossRef](#)] [[PubMed](#)]
4. Zong, Y.; Xu, S.; Matula, T.; Wan, M. Cavitation-Enhanced Mechanical Effects and Applications. In *Cavitation in Biomedicine: Principles and Techniques*; Wan, M., Feng, Y., Haar, G., Eds.; Springer: Dordrecht, The Netherlands, 2015; pp. 207–263. [[CrossRef](#)]
5. Unger, E.C.; Matsunaga, T.O.; McCreery, T.; Schumann, P.; Sweitzer, R.; Quigley, R. Therapeutic applications of microbubbles. *Eur. J. Radiol.* **2002**, *42*, 160–168. [[CrossRef](#)]
6. Goertz, D.E.; Todorova, M.; Mortazavi, O.; Agache, V.; Chen, B.; Karshafian, R.; Hynynen, K. Antitumor effects of combining docetaxel (taxotere) with the antivasular action of ultrasound stimulated microbubbles. *PLoS ONE* **2012**, *7*, e52307. [[CrossRef](#)]
7. Pu, C.; Chang, S.; Sun, J.; Zhu, S.; Liu, H.; Zhu, Y.; Wang, Z.; Xu, R.X. Ultrasound-mediated destruction of LHRHa-targeted and paclitaxel-loaded lipid microbubbles for the treatment of intraperitoneal ovarian cancer xenografts. *Mol. Pharm.* **2014**, *11*, 49–58. [[CrossRef](#)]
8. Gao, Y.; Wang, X.; Liu, P.; Yang, W.; Li, L.; Li, P.; Liu, Z.; Zhuo, Z. Microbubbles coupled to methotrexate-loaded liposomes for ultrasound-mediated delivery of methotrexate across the blood-brain barrier. *Int. J. Nanomed.* **2014**, *9*, 4899. [[CrossRef](#)] [[PubMed](#)]
9. Zhou, S.; Li, S.; Liu, Z.; Tang, Y.; Wang, Z.; Gong, J.; Liu, C. Ultrasound-targeted microbubble destruction mediated herpes simplex virus-thymidine kinase gene treats hepatoma in mice. *J. Exp. Clin. Cancer Res.* **2010**, *29*, 170–175. [[CrossRef](#)]
10. Dimcevski, G.; Kotopoulos, S.; Bjånes, T.; Hoem, D.; Schjøtt, J.; Gjertsen, B.T.; Biermann, M.; Molven, A.; Sorbye, H.; McCormack, E.; et al. A human clinical trial using ultrasound and microbubbles to enhance gemcitabine treatment of inoperable pancreatic cancer. *J. Control. Release* **2016**, *243*, 172–181. [[CrossRef](#)]
11. Lyon, P.C.; Gray, M.D.; Mannaris, C.; Folkes, L.K.; Stratford, M.; Campo, L.; Chung, D.Y.F.; Scott, S.; Anderson, M.; Goldin, R.; et al. Safety and feasibility of ultrasound-triggered targeted drug delivery of doxorubicin from thermosensitive liposomes in liver tumours (TARDOX): A single-centre, open-label, phase 1 trial. *Lancet Oncol.* **2018**, *19*, 1027–1039. [[CrossRef](#)]
12. Yu, H.; Xu, L. Cell experimental studies on sonoporation: State of the art and remaining problems. *J. Control. Release* **2014**, *174*, 151–160. [[CrossRef](#)] [[PubMed](#)]
13. Kinoshita, M.; Hynynen, K. Key factors that affect sonoporation efficiency in in vitro settings: The importance of standing wave in sonoporation. *Biochem. Biophys. Res. Commun.* **2007**, *359*, 860–865. [[CrossRef](#)] [[PubMed](#)]
14. Zhang, Y.; Azuma, T.; Sasaki, A.; Yoshinaka, K.; Takagi, S.; Matsumoto, Y. Ultrasound-mediated gene transfection: A comparison between cells irradiated in suspension and attachment status. *AIP Conf. Proc.* **2012**, *1481*, 481–487. [[CrossRef](#)]
15. Zhou, Q.; Chen, J.-L.; Chen, Q.; Wang, X.; Deng, Q.; Hu, B.; Guo, R.-Q. Optimization of transfection parameters for ultrasound/SonoVue microbubble-mediated hAng-1 gene delivery in vitro. *Mol. Med. Rep.* **2012**, *6*, 1460–1464. [[CrossRef](#)] [[PubMed](#)]
16. Eisenbrey, J.R.; Shraim, R.; Liu, J.-B.; Li, J.; Stanczak, M.; Oeffinger, B.; Leeper, D.B.; Keith, S.W.; Jablonowski, L.J.; Forsberg, F.; et al. Sensitization of Hypoxic Tumors to Radiation Therapy Using Ultrasound-Sensitive Oxygen Microbubbles. *Int. J. Radiat. Oncol. Biol. Phys.* **2018**, *101*, 88–96. [[CrossRef](#)]
17. Nande, R.; Greco, A.; Gossman, M.S.; Lopez, J.P.; Claudio, L.; Salvatore, M.; Brunetti, A.; Denvir, J.; Howard, C.M.; Claudio, P.P. Microbubble-assisted p53, RB, and p130 gene transfer in combination with radiation therapy in prostate cancer. *Curr. Gene Ther.* **2013**, *13*, 163–174. [[CrossRef](#)]
18. Karshafian, R.; Giles, A.; Burns, P.N.; Czarnota, G.J. Ultrasound-activated microbubbles as novel enhancers of radiotherapy in leukemia cells in vitro. In Proceedings of the IEEE International Ultrasonics Symposium, Rome, Italy, 20–23 September 2009; pp. 1792–1794. [[CrossRef](#)]
19. Karshafian, R.; Tchouala, J.I.N.; Al-Mahrouki, A.; Giles, A.; Czarnota, G.J. Enhancement of radiation therapy by ultrasonically-stimulated microbubbles in vitro: Effects of treatment scheduling on cell viability and production of ceramide. In Proceedings of the IEEE International Ultrasonics Symposium, San Diego, CA, USA, 11–14 October 2010; pp. 2115–2118. [[CrossRef](#)]
20. Al-Mahrouki, A.A.; Karshafian, R.; Giles, A.; Czarnota, G.J. Bioeffects of Ultrasound-Stimulated Microbubbles on Endothelial Cells: Gene Expression Changes Associated with Radiation Enhancement In Vitro. *Ultrasound Med. Biol.* **2012**, *38*, 1958–1969. [[CrossRef](#)]
21. Nofiele, J.I.T.; Karshafian, R.; Furukawa, M.; Al Mahrouki, A.; Giles, A.; Wong, S.; Czarnota, G.J. Ultrasound-Activated Microbubble Cancer Therapy: Ceramide Production Leading to Enhanced Radiation Effect In Vitro. *Technol. Cancer Res. Treat.* **2013**, *12*, 53–60. [[CrossRef](#)]
22. Al-Mahrouki, A.A.; Wong, E.; Czarnota, G.J. Ultrasound-stimulated microbubble enhancement of radiation treatments: Endothelial cell function and mechanism. *Oncoscience* **2015**, *2*, 944–957. [[CrossRef](#)]
23. Lammertink, B.H.A.; Bos, C.; van der Wurff-Jacobs, K.M.; Storm, G.; Moonen, C.T.; Deckers, R. Increase of intracellular cisplatin levels and radiosensitization by ultrasound in combination with microbubbles. *J. Control. Release* **2016**, *238*, 157–165. [[CrossRef](#)]

24. Al-Mahrouki, A.; Giles, A.; Hashim, A.; Kim, H.C.; El-Falou, A.; Rowe-Magnus, D.; Farhat, G.; Czarnota, G.J. Microbubble-based enhancement of radiation effect: Role of cell membrane ceramide metabolism. *PLoS ONE* **2017**, *12*, e0181951. [[CrossRef](#)]
25. Deng, H.; Cai, Y.; Feng, Q.; Wang, X.; Tian, W.; Qiu, S.; Wang, Y.; Li, Z.; Wu, J. Ultrasound-Stimulated Microbubbles Enhance Radiosensitization of Nasopharyngeal Carcinoma. *Cell. Physiol. Biochem.* **2018**, *48*, 1530–1542. [[CrossRef](#)]
26. McCorkell, G.; Nakayama, M.; Feltis, B.; Piva, T.; Geso, M. Ultrasound-Stimulated Microbubbles Enhance Radiation-Induced Cell Killing. *Ultrasound Med. Biol.* **2022**, *48*, 2449–2460. [[CrossRef](#)] [[PubMed](#)]
27. Dos Santos, M.; Paget, V.; Ben Kacem, M.; Trompier, F.; Benadjaoud, M.A.; François, A.; Guipaud, O.; Benderitter, M.; Milliat, F. Importance of dosimetry protocol for cell irradiation on a low X-rays facility and consequences for the biological response. *Int. J. Radiat. Biol.* **2018**, *94*, 597–606. [[CrossRef](#)] [[PubMed](#)]
28. Goretzki, P.; Frilling, A.; Simon, D.; Roehrer, H.-D. Growth regulation of normal thyroids and thyroid tumors in man. In *Hormone-Related Malignant Tumors*; Springer: Berlin/Heidelberg, Germany, 1990; pp. 48–63.
29. Takahashi, T.; Nau, M.M.; Chiba, I.; Birrer, M.J.; Rosenberg, R.K.; Vinocour, M.; Levitt, M.; Pass, H.; Gazdar, A.F.; Minna, J.D. p53: A Frequent Target for Genetic Abnormalities in Lung Cancer. *Science* **1989**, *246*, 491. [[CrossRef](#)]
30. Promega Corporation. *CellTiter 96®AQueous One Solution Cell Proliferation Assay*; Promega Corporation: Madison, WI, USA, 2012.
31. Lantheus DEFINITY®RT (Perflutren Lipid Microsphere) Injectable Suspension. 2023. Available online: <https://www.definityimaging.com/sites/default/files/pdf/definity-rt-pi.pdf> (accessed on 7 August 2023).
32. Laerd Statistics. Testing for Normality Using SPSS Statistics When You Have Only One Independent Variable. 2018. Available online: <https://statistics.laerd.com/spss-tutorials/testing-for-normality-using-spss-statistics.php> (accessed on 23 May 2023).
33. Gignac, G.E. How2statsbook 2019. Available online: <https://sites.google.com/site/how2statsbook1/Table%20of%20Contents%20-%202019.pdf?attredirects=0&d=1> (accessed on 23 May 2023).
34. Bakeman, R. Recommended effect size statistics for repeated measures designs. *Behav. Res. Methods* **2005**, *37*, 379–384. [[CrossRef](#)]
35. Blanca, M.J.; Alarcón, R.; Arnau, J. Non-normal data: Is ANOVA still a valid option? *Psicothema* **2017**, *29*, 552–557. [[CrossRef](#)] [[PubMed](#)]
36. One-Way ANOVA—Violations to the Assumptions of This Test and How to Report the Results | Laerd Statistics n.d. Available online: <https://statistics.laerd.com/statistical-guides/one-way-anova-statistical-guide-3.php> (accessed on 9 October 2020).
37. Lee, H.; Kim, H.; Han, H.; Lee, M.; Lee, S.; Yoo, H.; Chang, J.H.; Kim, H. Microbubbles used for contrast enhanced ultrasound and theragnosis: A review of principles to applications. *Biomed. Eng. Lett.* **2017**, *7*, 59–69. [[CrossRef](#)]
38. Znych, A.; Fournier, L.; Chauvierre, C. Nanomedicine progress in thrombolytic therapy. *Biomaterials* **2020**, *258*, 120297. [[CrossRef](#)]
39. Lattwein, K.R.; Shekhar, H.; Kouijzer, J.J.P.; van Wamel, W.J.B.; Holland, C.K.; Kooiman, K. Sonobactericide: An Emerging Treatment Strategy for Bacterial Infections. *Ultrasound Med. Biol.* **2020**, *46*, 193–215. [[CrossRef](#)]
40. Panje, C.M.; Wang, D.S.; Willmann, J.K. Ultrasound and Microbubble-Mediated Gene Delivery in Cancer: Progress and Perspectives. *Investig. Radiol.* **2013**, *48*, 755–769. [[CrossRef](#)] [[PubMed](#)]
41. Deprez, J.; Lajoinie, G.; Engelen, Y.; De Smedt, S.C.; Lentacker, I. Opening doors with ultrasound and microbubbles: Beating biological barriers to promote drug delivery. *Adv. Drug Deliv. Rev.* **2021**, *172*, 9–36. [[CrossRef](#)] [[PubMed](#)]
42. Fournier, L.; De La Taille, T.; Chauvierre, C. Microbubbles for human diagnosis and therapy. *Biomaterials* **2023**, *294*, 122025. [[CrossRef](#)]
43. Padilla, F.; Puts, R.; Vico, L.; Guignandon, A.; Raum, K. Stimulation of Bone Repair with Ultrasound. In *Therapeutic Ultrasound*; Escoffre, J.-M., Bouakaz, A., Eds.; Springer International Publishing: Cham, Switzerland, 2016; pp. 385–427. [[CrossRef](#)]
44. Whitney, N.P.; Lamb, A.C.; Louw, T.M.; Subramanian, A. Integrin-Mediated Mechanotransduction Pathway of Low-Intensity Continuous Ultrasound in Human Chondrocytes. *Ultrasound Med. Biol.* **2012**, *38*, 1734–1743. [[CrossRef](#)]
45. Hu, B.; Zhang, Y.; Zhou, J.; Li, J.; Deng, F.; Wang, Z.; Song, J. Low-Intensity Pulsed Ultrasound Stimulation Facilitates Osteogenic Differentiation of Human Periodontal Ligament Cells. *PLoS ONE* **2014**, *9*, e95168. [[CrossRef](#)]
46. Gilmore, A.P. Anoikis. *Cell Death Differ.* **2005**, *12*, 1473–1477. [[CrossRef](#)] [[PubMed](#)]
47. Zhong, X.; Rescorla, F.J. Cell surface adhesion molecules and adhesion-initiated signaling: Understanding of anoikis resistance mechanisms and therapeutic opportunities. *Cell. Signal.* **2012**, *24*, 393–401. [[CrossRef](#)]
48. Simpson, C.D.; Anyiwe, K.; Schimmer, A.D. Anoikis resistance and tumor metastasis. *Cancer Lett.* **2008**, *272*, 177–185. [[CrossRef](#)]

**Disclaimer/Publisher’s Note:** The statements, opinions and data contained in all publications are solely those of the individual author(s) and contributor(s) and not of MDPI and/or the editor(s). MDPI and/or the editor(s) disclaim responsibility for any injury to people or property resulting from any ideas, methods, instructions or products referred to in the content.